

EXPERIMENTAL STUDY OF THE TRANSVERSE MODE COUPLING INSTABILITY WITH SPACE-CHARGE AT THE CERN SPS

X. Buffat*, H. Bartosik, CERN, Geneva, Switzerland

Abstract

Past studies on the Transverse Mode Coupling Instability (TMCI) suggested that it can be suppressed in the presence of space-charge forces. Recent developments in this field show that for higher strength, space-charge forces lead to other types of instabilities. We investigate the characteristics of these instabilities by means of stability threshold measurements at the CERN SPS for various intensities, longitudinal and transverse emittances. These observations are compared to numerical tracking simulations.

INTRODUCTION

The Transverse Mode Coupling Instability (TMCI) often limits the maximum bunch intensity in synchrotrons [1]. While it is expected that weak space-charge forces can mitigate the TMCI [2], strong enough space-charge fields may give rise to new mode coupling instabilities [3, 4]. We present experimental studies aiming at demonstrating the existence of these instabilities and determine the dependence on the most relevant machine and beam parameters at the CERN SPS.

Instabilities with strong space-charge are predicted by linearised models which do not allow for quantitative comparison with experimental data, due to the lack of modelling for Landau damping caused by the tune spread driven by space-charge forces. We therefore use macroparticle tracking simulations for comparison with experimental data. The tracking through the lattice is performed using SixtrackLib [5] based on the thin lens optics of the SPS [6] featuring multipole errors in the dipoles and quadrupoles up to 7th order. Self-consistent space-charge field computations are performed at discrete points around the machine using PyPIC [7]. Both lattice and space-charge computations are accelerated on GPU. The impact of the wake fields is computed with PyHEADTAIL [8] using the 2018 impedance model of the SPS [9]. The machine, beam and numerical parameters are listed in Tab. 1.

INSTABILITY THRESHOLD

A series of experiments were conducted at the SPS, during which a single bunch with different properties was injected and kept at flat bottom allowing for a monitoring of the evolution of the beam properties and assess in particular the transverse stability threshold. The experimental procedure consisted in varying the transverse emittances by approaching the integer tune and then the coupling

Table 1: Machine, Beam and Numerical Parameters

Energy [GeV]	26
Bunch intensity [10^{11} p/b]	1.5 to 2.4
Trans. norm. emit. [μm]	0.5 to 6
Long. emit. [eVs]	0.25 to 0.4
H/V tune	26.15 / 26.22
H/V chromaticity	3.0/2.0
H/V 2 nd order chroma. [10^2]	2.8/1.2
H/V 3 rd order chroma. [10^5]	-5.0/3.2
Synchrotron tune [10^{-4}]	4.2
RF Voltage (200MHz) [MV]	1
RF Voltage (800MHz) [MV]	0.1
Nb. turns	$1.3 \cdot 10^5$
Nb. macroparticles	10^6
Nb. slices for wake	500
Nb. slices for PIC	50
PIC grid size	128x128
Number of space-charge kicks	540

resonance at the flat bottom of the PS, in order to obtain round beams yet maintaining the same intensity and longitudinal emittance. By doing so, the strength of the space-charge forces is varied keeping the strength of the wake fields constant. The operation was repeated for different intensities and longitudinal emittances, obtained with dedicated setup in the PSB.

We use the intensity transmission through the flat bottom of the SPS to characterise the stability of the beam. The experimental data as well as the results of simulations are shown in Fig. 1. The experimental data (dots) on the top plot corresponds to configurations featuring a measured longitudinal emittance of 0.3 eVs but varying intensities and transverse emittances. The simulations with space-charge (solid lines) are slightly pessimistic with respect to the observations, yet the dependence with the transverse emittance is well described. There is a significant uncertainty related to the longitudinal distribution, since it is measured at the PS flat top, before the phase-space rotation that occurs right before the injection into the SPS [10]. As discussed later, the instability may develop within tens to hundreds of turns following the injection into SPS, such that the longitudinal distribution is not yet fully matched. It is therefore expected that the simulations with 0.3 eVs are pessimistic. The agreement is significantly better with 0.4 eVs. The remaining differences may be attributed to the uncertainty on the measured transverse emittance ($\approx 20\%$).

* xavier.buffat@cern.ch

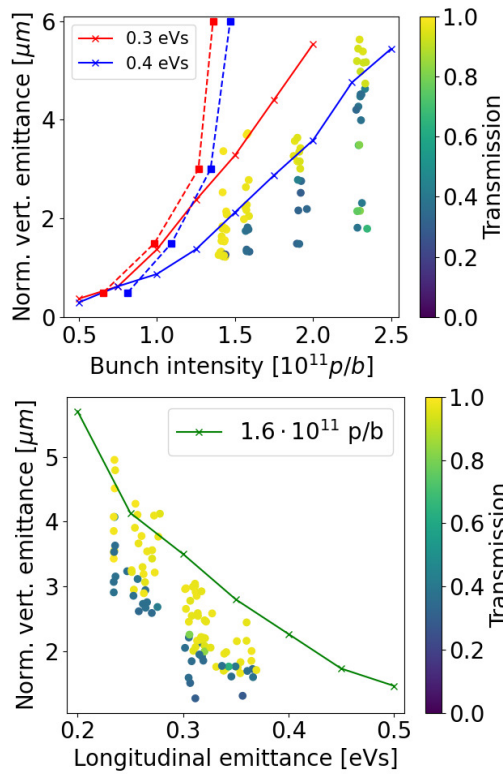


Figure 1: The coloured dots represent the intensity transmission measured through the flat bottom of the SPS with various intensity and transverse emittance at a constant longitudinal emittance of 0.3 eVs (top) and with various longitudinal and transverse emittances at constant intensity of $1.6 \cdot 10^{11}$ protons per bunch. The lines show the instability threshold obtained in tracking simulations with space-charge (solid) and without (dashed).

Simulations without space-charge (dashed lines) exhibit a weak dependence of the instability threshold on the transverse emittance, which is not compatible with the experimental data. This comparison suggests that transverse Landau damping due to the lattice non-linearities is rather weak. This was confirmed experimentally by a measurement of the transverse detuning terms, yielding a r.m.s. tune spread of about $2 \cdot 10^{-5}$ for the largest emittance considered here. This tune spread may have a stabilising effect close to the threshold, however the imaginary tune shift grows rapidly to much larger values above the threshold (see below). The significant increase of the measured intensity limit with larger transverse emittance could therefore not be attributed to additional Landau damping caused by lattice non-linearities only.

We note that the instability threshold does not correspond to a fixed limit in space-charge tune shift. In fact, the stable configurations with highest space-charge tune shifts are achieved with low bunch intensities. For example with a longitudinal emittance of 0.4 eVs, the maximum vertical

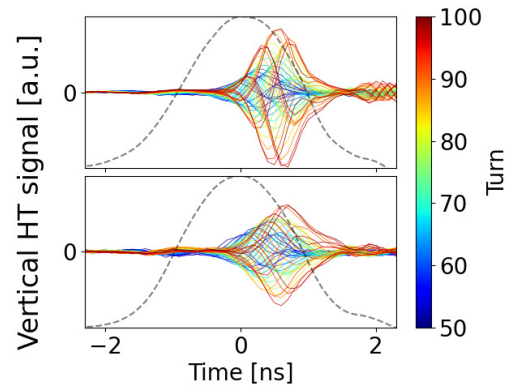


Figure 2: HT signal measured by a vertical wideband pickup during the first 50 turns after injection into the SPS. The dashed black line show the longitudinal line density measured by same pickup. The intensity is $2.3 \cdot 10^{11}$ in both configurations, but the emittance is far from the threshold for the top plot ($1.8 \mu\text{m}$) and close to it for the bottom plot ($4.1 \mu\text{m}$).

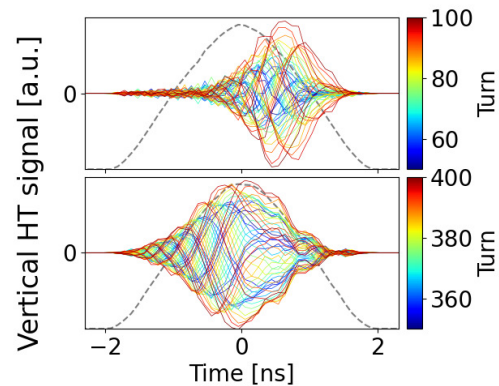


Figure 3: Vertical HT signal obtained with tracking simulation with space-charge (top) and without space-charge (bottom) with the parameters listed in Tab. 1, an intensity of $2.3 \cdot 10^{11}$, transverse emittances of $1.8 \mu\text{m}$ and a longitudinal emittance of 0.4 eVs. The dashed black line show the longitudinal line density.

shift is estimated at 0.09 at the instability threshold with a high intensity ($2.5 \cdot 10^{11}$) and 0.16 with a low intensity ($1 \cdot 10^{11}$).

HEAD TAIL SIGNAL

The difference signal measured by vertical wideband pickup, known as the HT signal, is shown for few consecutive passages of the bunch in Fig. 2. The two configurations shown correspond to high intensities with an emittance close and far from the instability threshold. Both signals feature a strong asymmetry in the oscillation of the head (negative times) and the tail (positive times). The configuration close to the threshold, i.e. with weakest space-charge

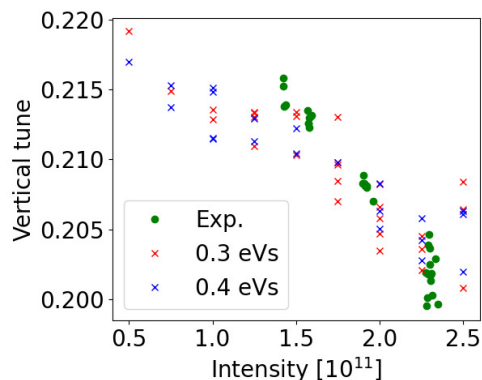


Figure 4: Tune of the unstable oscillations obtained with an interpolated FFT of the turn-by-turn vertical position. Tracking simulations are represented by crosses with two different longitudinal emittances. The experimental data obtained with the BBQ are shown with green dots.

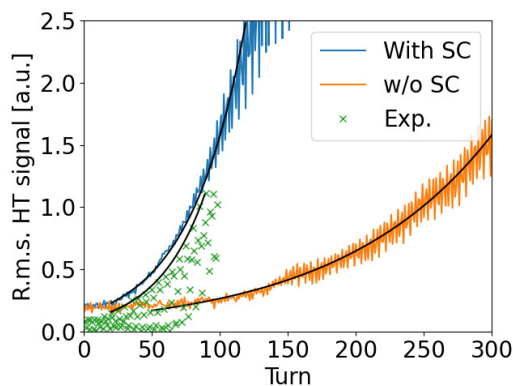


Figure 5: Amplitude of the transverse oscillation obtained from the measured HT signal for the first hundreds of turns following injection into the SPS. The green crosses show the experimental data corresponding to the top plot in Fig. 2. The blue and orange lines show the results of tracking simulations with and without space-charge with the same machine and beam parameters. The black lines show the result of exponential fits, yielding 42 and 112 turns for the simulation with and without space-charge respectively. The measured growth time is 36 turns.

forces, features intrabunch waves of slightly lower frequency.

The configuration with a low emittance can be compared directly to the simulated HT signals in Fig. 3. The signals obtained with space-charge is extremely similar, featuring notably the same asymmetry between the head and the tail. The same simulation without space-charge reveals a mode with a different structure with a reduced asymmetry.

TUNE AND GROWTH RATE

The tune of the unstable mode of oscillation obtained from experimental data and simulations are shown in Fig. 4.

We note that as well as to simulations exhibit a non-linear behaviour of the tune for intensities below $1.5 \cdot 10^{11}$ which could not be probed experimentally. Above this intensity, the behaviour is rather linear in both the experimental data and the simulation, yet the slope is about 15% higher in the experimental data. In both simulations and experimental data, the impact of the transverse emittance remains within the error bar on the tune measurement. The latter is pretty large due to the fast nature of the instability.

The evolution of the amplitude of the oscillation for one of the instabilities observed with high intensity is shown in Fig. 5, along with the equivalent observable from simulations with and without space-charge. The growth rate observed in simulations with space-charge is fully compatible with the observations, whereas simulations without space-charge exhibit an instability slower by a factor 2.

CONCLUSION

We have compared the instability threshold, HT signal, coherent tune and growth rate of instabilities measured at the injection into the SPS to those predicted by tracking simulations featuring self-consistent computation of the space-charge forces and by tracking simulations without space-charge. A good agreement is found with simulation featuring space-charge, whereas the dependence of the instability threshold on the transverse emittance, the HT signal as well as the growth rate are not reproduced in simulation without space-charge. These observations show that space-charge forces do have a significant impact on the TMCI threshold. This was not observed in past studies during which the transverse emittances were expected to follow brightness curves defined by various mechanisms in the injector chain, but were not monitored [11]. In the meantime, various improvements in the frame of the LHC Injector Upgrade [12] have enabled the study presented here.

The increase of the instability threshold with the transverse emittance could not be explained by the corresponding increase of the transverse tune spread due to lattice non-linearities. In addition the space-charge driven tune spread is expected to increase with lower emittance, such that Landau damping driven by space-charge forces can also not explain the experimental observations on their own. This implies the existence of an instability mechanism whose strength increases with the space-charge forces, such as those predicted in [3, 4]. The HT signal is also compatible with the one predicted by the linear model [4].

ACKNOWLEDGEMENTS

We would like to warmly thank S. Albright, F. Asvesta, M. Coly, H. Damerau, A. Huschauer, A. Lasheen, G. Papotti, B. Salvant and N. Triantafyllou as well as the PSB, PS and SPS operation crews for their help in the execution of these experimental studies.

REFERENCES

- [1] A.W. Chao, “Physics of Collective Beams Instabilities in High Energy Accelerators”, New York, USA: Wiley, 1993.
- [2] M. Blaskiewicz, “Fast head-tail instability with space charge”, *Phys. Rev. ST Accel. Beams*, vol. 1, p. 044201, 1998. doi:10.1103/PhysRevSTAB.1.044201
- [3] Y.H. Chin, *et al.*, “Two particle model for studying the effects of space-charge force on strong head-tail instabilities”, *Phys. Rev. Accel. Beams*, vol. 19, p. 014201, 2016. doi:10.1103/PhysRevAccelBeams.19.014201
- [4] X. Buffat, *et al.* “Description of beam instabilities in synchrotron with wakefields and space charge forces using the circulant matrix model”, *Phys. Rev. Accel. Beams*, vol. 24, p. 060101, 2021. doi:10.1103/PhysRevAccelBeams.24.060101
- [5] SixTrackLib, <https://github.com/SixTrack/sixtracklib>
- [6] CERN Super Proton Synchrotron Optics Repository, <https://acc-models.web.cern.ch/acc-models/sps/>
- [7] GitHub - PyCOMPLETE/PyPIC: PIC codes at cern, <https://github.com/PyCOMPLETE/PyPIC>
- [8] GitHub - PyCOMPLETE/PyHEADTAIL: CERN PyHEADTAIL macro-particle code for simulating beam dynamics in particle accelerators with collective effects. <https://github.com/PyCOMPLETE/PyHEADTAIL>
- [9] CERN impedance webpage, <https://impedance.web.cern.ch/>
- [10] A. Lasheen *et al.*, “Improvement of the longitudinal beam transfer from the PS to the SPS at CERN”, in *Proc. IPAC’19*, Vancouver, Canada, April 2019, pp. 3060–3063. doi:10.18429/JACoW-IPAC2018-THPAF041
- [11] H. Bartosik, “Beam dynamics and optics studies for the LHC injectors upgrade”, Ph.D. thesis, Technische Universität Wien, 2013
- [12] H. Damerau, *et al.*, eds., “LHC Injectors Upgrade, Technical Design Report”, (CERN, Geneva, Switzerland, 2014) <http://cds.cern.ch/record/1976692>